Pak. J. Bot., 55(4): 1229-1243, 2023. DOI: http://dx.doi.org/10.30848/PJB2023-4(18)

OSMOREGULATION MEDIATED BY STRUCTURAL AND FUNCTIONAL FEATURES IN *CENCHRUS CILIARIS* L. UNDER SALINE CONDITIONS

SHAMEEM KAUSAR, FAROOQ AHMAD AND MANSOOR HAMEED

Department of Botany, University of Agriculture Faisalabad, Faisalabad 38040, Pakistan
Corresponding author's email: farooqbot@yahoo.com

Abstract

Cenchrus ciliaris L. (buffel grass) is a forage grass widely distributed in saline and arid regions of Pakistan. Populations of *C. ciliaris* were collected from ten diverse habitats to evaluate their response to salinity stress. Three populations, Lal Suhanra (LS), Ladamsar (LD) and Derawar Fort (DF), were collected from highly saline habitats. The populations collected from low saline habitats were Qila Nawab Din (QN), Darbar Anayat Shah (DA), Nathia Galli (NG) and Kanhatti Garden (KG), while non-saline were Jaba (JB), Chok Azam (CA) and Khanewal (KH). Morpo-anatomical and physiological traits varied greatly in differently adapted populations. Population collected from the highest salinity (Lal Suhanra) showed the lowest root dry weight. Concentration of proline content and shoot K^+ was the highest. Endodermal thickness in roots was the maximum, while size of bulliform cells, leaf sheath thickness and size of metaxylem vessels were the minimum in Lal Suhanra population. Plants collected from highly saline Ladamsar were the shortest in height with minimum root and shoot fresh weight and shoot dry weight. Root Na^+ was the maximum in this population, while the largest endodermal cells and broadest xylem vessels were observed in Ladamsar population. Stem anatomical features like epidermal thickness, metaxylem area and vascular bundle area, leaf traits like lamina thickness and cortical cell area, and leaf sheath parameters like leaf sheath thickness, epidermal thickness and cortical cell area were the maximum in Ladamsar population. Plasticity is exceptionally high in all *C. ciliaris* populations, which might be the reason for its wide distributional range in a variety of habitats. Because of its heterogenic nature, *C. ciliaris* is among the most suitable species for re-vegetation of saline arid, disturbed and Narran lands.

Key words: Salinity, Bulliform cells, Buffel grass, Anatomical adaptations, Aerenchyma.

Introduction

Salinization limits crop growth and yield in arid areas worldwide (Safdar *et al*., 2019; Shrivastava & Kumar, 2015). Salinity has become a major reason for degradation of land all over the world (Ma *et al*., 2015**).** About 800 million hectares (mha) of land is salt affected due to poor agriculture land practices (Shrivastava & Kumar, 2015). The main cause of salinity is high evaporation and low precipitation in these arid regions (Hussain *et al*., 2019), resulting in delayed germination, decreased growth and yield in these plants (Negrao *et al*., 2017). Salinity negatively affects growth and physiology of plants, which is mainly due to oxidative stress and ionic imbalance (Ma *et al*., 2017). This directly affects growth and biomass production of plant species (Xu & Mou, 2015). Modifications in anatomical characteristics under saline conditions include increased succulence due to high proportion of storage parenchyma. Reduced stomatal density and size, and reduced leaf area minimize transpiration rate (Mumtaz *et al*., 2021). Proportion of vascular tissues generally increased in more tolerant species, which involve in better conduction of solutes and photosynthates (Naz *et al*., 2018).

Halophytic grasses can tolerate salinity, either by accumulating salts in their plant organs or by excreting salts outside the plant body (Hameed *et al*., 2013). Plants tolerate salinity by different mechanisms. Toxic ions initially restricted at root level, mainly due to root modifications like thick epidermis, lignified cortical parenchyma and thicker inner tangential walls of endodermis (Robbins *et al*., 2014). When salt enters in plant body, excess salt may either dump in inert places like vacuoles or older leaves, or excrete through salt hairs, glands and micro-hairs (Fatima *et al.,* 2021).

Cenchrus ciliaris L. is a perennial fodder grass, distributed in saline and arid habitats all over Pakistan (Mansoor *et al*., 2019). It is widely grown in tropical areas around the world due to its ability to withstand over grazing pressure (Al-Dakheel *et al*., 2015b). *Cenchrus ciliaris* is very suitable for all soil types and has the ability to quickly invade and survive in saline and arid conditions (Khan *et al*., 2017). Due to its high palatability and rich in nutrients, it is considered suitable for livestock forage production in these areas (Al-Dakheel *et al*., 2015b).

The present study focused on anatomical and physiological features of naturally adapted populations of *C. ciliaris* along salinity gradient. It was hypothesized that differently adapted populations of *C. ciliaris* must develop xeric features and must have variation in structural and functional traits, which enable these species to cope with physiological droughts caused by salinity stress. The research objectives were a) identification of structural and functional features suitable for salinity tolerance, and b) correlation of growth attributes with soil physicochemical and anatomical traits.

Materials and Methods

Ten Populations of *Cenchrus ciliaris* L. were collected from different areas in the Punjab, Pakistan. The collection sites were: Ladamsar (ECe=32.7 dS/m; all values of EC in parentheses are presented as dS/m), Derawar Fort (ECe=21.7), Lal Suhanra (ECe=40.0), Nathia Galli (ECe=4.7), Qila Nawab Din (ECe=7.3), Kanhatti Garden (ECe=4.4), Darbar Anayat Shah (ECe=4.8), Khanewal (ECe=1.3), Chok Azam (ECe=1.9) and Jaba (ECe=2.0) (Fig. 1).

Lal Suhanra (ECe 40 dS m^{-1}, coordinates 29°27'54.12"N 71°58'17.28"E, elevation 129 m a.s.l.): Salt affected uncultivated area, dominated by *Octhochloa compressa* and some dicot halophytic species.

Ladam Sir (ECe 32.7 dS m^{-1}, coordinates 29°21'00.33"N, 71°42'11.80"E, elevation 126 m a.s.l.): Heavily salt affected area in the Cholistan Desert.

Derawar Fort (ECe 21.7 dS m^{-1}, coordinates 28°46'04.81"N, 72°26'00.07"E, elevation 117 m a.s.l.): Sandy soil and muddy flats, heavily salt-affected area.

Qila Nawab Din (ECe 7.31 dS m^{-1}, coordinates 28°25'0778"N, 70°18'13.54"E, elevation 121 m a.s.l.): Cholistan desert flats and sand dunes with sandy soil.

Darbar Anayat Shah (ECe 4.83 dS m^{-1}, coordinates 30°58'12.17"N, 70°56'31.12"E, elevation 147 m a.s.l.): Hot and dry environment with sandy soil and scattered sand dunes.

Nathia Gali (ECe 4.64 dS m^{-1}, coordinates 34°04'22.8"N, 73°22'52.45"E, elevation 2315 m a.s.l.): Along road side in the mountainous region with dense vegetation.

Kanhatti Garden (ECe 4.34 dS m^{-1}, Coordinates 32°40'35.60"N, 72°14'52.61"E, elevation 625 m a.s.l.): Sedimentary rocks in the Salt Range, characterized by gravel stones and scrub vegetation.

Jaba (ECe 1.99 dS m^{-1}, coordinates 33°53'34.04"N, 73°20'20.84"E, elevation 763 m a.s.l.): Mountain slopes along the road, dominated by *Acacia modesta* and *Olea ferruginea.*

Chok Azam (ECe 1.94 dS m^{-1}, coordinates 30°57'51.67"N, 71°12'28.18"E, elevation 149 m a.s.l.): Margin of the Thal Desert with scattered small sand dunes.

Khanewal (ECe 1.25 dS m^{-1}, coordinates 30°17'11.10"N, 71°55'55.29"E, elevation 136 m a.s.l.): Forest plantation, mainly of *Acacia nilotica, Dalbergia sissoo* and *Eucalyptus camaldulensis*

Fig. 1. Habitat description and pictorial presentation of collection sites of *Cenchrus ciliaris* L. populations.

Soil analysis: To analyze soil physicochemical characteristics, soil from rhizosphere of plants at the depth of 16 cm was taken from each habitat. Six plants (replications) of average size were collected from each site. The pH and electrical conductivity (ECe) was estimated by using pH/EC meter (WTW series Ino Lab pH/Cond 720, USA). Soil texture was determined by using USDA texture triangle method (Estefan *et al*., 2013). Soil Na^+, K^+, Ca^{2+} and Mg^{2+} were determined by using flame photometer (Jenway, PFP-7, UK). For saturation percentage, dry soil (200 g) was taken into a porcelain petri dish and known amount of water was added to form the soil paste (Estefan *et al*., 2013). Organic matter (% age) was measured by using the protocol devised by Sims & Haby (1971).

Morphological attributes: Whole plant was uprooted carefully using soil auger (10 cm dia.). The plants were immediately weighed by Ohaus compact portable digital balance. The plants were kept in oven at 65°C for 6 days till the constant weight obtained, and plant dry weight was taken on a digital balance. Shoot length was measured from the stem base to the top and root length from base of the stem to end of the roots.

Organic osmolytes: Free proline was determined by the method of Bates *et al*., (1973). Fresh plant samples were homogenized with sulfo-salicylic acid, filtered and then added to ninhydrin solution. Absorbance was recorded at 520 nm using spectrophotometer after one hour (Hitatchi, 220, Japan).

The method of Grieve & Grattan (1983) was used to estimate the glycine betaine content. Fresh leaf sample (1.0g) was ground in10 mL solution of 0.5% toluene and filtered it. The filtrate (1.0 Ml) was then mixed with 1 mL 2N H_2SO_4. After this, 0.5 mL supernatant was added to potassium tri-iodide (0.2 mL), mixture was shaken and cooled in an ice bath for 90 min. Then added ice cooled distilled water (2.8 mL) and 1,2 di-chloroethane (6 mL) in each test tube. In test tube, two layers were formed. By using spectrophotometer, optical density was measured at 365 nm of the upper layer.

Total soluble sugars were determined according to the method of Yemm & Willis (1954). Plant material was extracted in 80% ethanol solution. Freshly prepared anthrone reagent was used and optical density was recorded at 625 nm on spectrophotometer (Hitatchi, 220, Japan).

Ionic content: Dried shoot and root materials were digested separately with sulphuric acid and hydrogen per oxide for analyzing nutrients like Na^+, Ca^{2+} and K^+ with a flame photometer (Model 410, Sherwood Scientific Ltd., Cambridge, UK) following Wolf (1982).

Anatomical characteristics: For anatomical studies, plant material was preserved in the FAA (formalin acetic alcohol) solution. Thin sections of root, stem and leaves were cut by free-hand sectioning method for anatomical study of tissues and cells. Permanent slides were prepared by serial dehydration by ethanol grades (30%, 50%, 70%, 90% and 100% ethanol) for 10 to 15 minutes in each grade. The selected sections were stained by a double-staining procedure using safranin and fast green dyes. Photographs of stained slides were taken by using light microscope (Nikon 1004, Japan). Measurement of the different anatomical features was taken with the help of ocular micrometer after calibration with a stage micrometer.

Statistical analysis

Data were subjected to statistical analysis using analysis of variance (ANOVA) technique. Moreover, the data were subjected to the multivariate analysis (PCA), by using an R statistical software (R Core Team, 2019) to assess the relationship between studied traits. Pearson's correlation coefficient was calculated by using Microsoft Excel.

Results

Soil physicochemical characteristics: The maximum soil electrical conductivity (ECe) was observed in highly saline LS (40.0 dS m^{-1}), while the minimum ECe was noted in non-saline KH (1.3 dS m^{-1}). Soil pH was the maximum at highly saline LD (8.7) and DF (8.6), while the minimum pH was observed in highly saline LS (7.9) and low saline NG (7.9). Non-saline KH showed the maximum K^+ (320.3 mg kg^{-1}). Highly saline LS showed the minimum K^+ (160.8 mg kg^{-1}). The maximum Na^+ (4225.4 mg kg^{-1}) was observed in highly saline LS, and the minimum was in non-saline KH (62.1 mg kg^{-1}). Non-saline habitat KH showed the maximum Ca^{2+} (62.6 mg kg^{-1}), while the minimum was observed in highly saline habitat LS (12.6 mg kg^{-1}). Soil Mg^{2+} was the maximum at highly saline habitat LS (0.536 mg kg^{-1}) and the minimum was noted in non-saline habitat KH (0.24 mg kg^{-1}). Organic matter was the maximum at highly saline habitat LD (1.18 %), and its minimum was in low saline habitat QN (0.41%). The maximum saturation percentage was observed in non-saline habitat JB (31.0%) whereas, minimum saturation percentage was noted in highly saline habitat LD (13.0 %) (Table 1).

Morphological parameters: The maximum shoot length (40.5cm) was observed in low saline NG and the minimum (15.9 cm) in highly saline LD. The maximum root length (10.3 cm) was recorded in non-saline CA and the minimum in DF (4.5 cm) and QN (4. 4 cm). The maximum root fresh weight (2.7 g), shoot fresh weight (30.6 g) and shoot dry weights (6.2 g) was observed in low saline NG. The minimum shoot fresh weight (12.3 g) was noted in highly saline LD and root fresh weight (1.2 g) in LD and (1.1 g) in low saline QN. The minimum shoot dry weight (2.5 g) was noted in highly saline LS and LD. The maximum root dry weight (0.9g) was recorded in KH, JB and low saline NG. The minimum root dry weight (0.5 g) was noted in LS (Table 1).

Table 1. Soil physicochemical characteristics of the collection sites of *Cenchrus ciliaris* L.

	High saline			Low saline				Non-saline		
	LS	**LD**	**DF**	**QN**	**DA**	**NG**	**KG**	**JB**	**CA**	**KH**
	Soil physicochemical attributes									
Texture	LoS	FnS	FnS	SLo	FnS	SCL	SLo	SLo	LoS	SLo
OEC (dS m^{-1})	40.0a	32.7b	21.7c	7.3d	4.8e	4.7e	4.4f	2.0g	1.9h	1.3i
OpH	7.9e	8.7a	8.6a	8.3b	8.1d	7.9e	8.1d	8.0d	8.2c	8.2c
OK (mg kg^{-1})	160.8g	180.4f	180.5f	260.1b	210.5d	200.2e	180.6f	222.4c	200.2e	320.3a
ONa (mg kg^{-1})	4225.4a	3963.2b	2731.6c	867.6d	297.9e	213.9g	242.6f	82.7h	73.6i	62.1j
OCa (mg kg^{-1})	12.6j	18.9h	14.8i	20.8g	28.5e	26.2f	32.6d	52.3c	54.2b	62.6a
OMg (mg kg^{-1})	0.536a	0.425b	0.416c	0.231d	0.154e	0.124f	0.114g	0.96h	0.54i	0.24j
OOM (%)	0.83c	1.18a	0.69`d	0.41g	0.55f	0.83c	0.97b	0.73d	0.63e	0.76d
OSP (%)	20.0d	13.0i	14.0h	15.0g	18.0f	26.0c	24.0d	31.0a	19.0e	28.0b
	Morphological traits									
MSL (cm)	16.5g	15.9h	19.7f	19.9f	27.5d	40.5a	32.3b	19.2f	28.5c	24.2e
MRL(cm)	5.7f	5.5f	4.5g	4.4g	9.2b	9.4b	6.4e	8.3c	10.3a	7.4d
MSF (g)	13.2g	12.3h	17.5f	17.2f	22.3d	30.6a	26.8b	17.4f	23.6c	20.8e
MRF(g)	1.4e	1.2f	1.3e	1.1f	2.4b	2.7a	1.5d	1.7c	1.8c	1.5d
MSD (g)	2.7h	2.5i	3.5g	3.4g	4.5d	6.2a	5.4b	3.8f	4.8c	4.2e
MRD (g)	0.5e	0.6d	0.7c	0.6d	0.8b	0.9a	0.8b	0.9a	0.6d	0.9a
	Physiological traits									
Pro (µmol g^{-1} fw)	99.87a	91.58c	96.19b	50.34g	54.23f	56.25e	59.41d	14.10i	13.25j	15.32h
GB (µmol g^{-1} dw)	110.21c	115.23b	119.25a	70.61g	82.42f	93.45e	96.54d	20.51j	23.62i	25.36h
TSS (µmol g^{-1} fw)	50.68c	55.23b	59.42a	30.61g	36.27e	35.21f	39.95d	21.67j	24.37i	25.63h
SNa (mg g^{-1} dw)	72.35c	57.32b	58.75a	27.57g	35.63d	33.33e	31.04f	19.72j	21.25i	25.33h
RNa (mg g^{-1} dw)	93.54c	84.74a	76.22b	45.27e	44.15f	47.25d	42.32g	22.31i	23.22h	20.21j
SCa (mg g^{-1} dw)	23.99c	27.54b	30.71a	15.44e	17.64d	12.09h	14.84f	11.25i	13.23g	15.21e
RCa (mg g g^{-1} dw)	19.99a	17.54c	18.71b	14.44d	12.64e	11.64f	14.84d	10.21g	9.84h	12.36e
SK (mg g^{-1} dw)	12.22i	13.56h	15.24g	23.24d	25.45c	29.75b	30.15a	13.75h	16.42f	19.35e
RK (mg g^{-1} dw)	15.25g	18.23f	20.21e	25.24d	27.23c	28.75b	32.42a	10.75i	9.31j	12.24h

FnS-Fine sand, SLo-Sandy loam, SCL-sandy clay loam; LoS-Loamy sand

Collection sites: Lal Suhanra (LS), Ladamsar (LD), Derawar Fort (DF), Qila Nawab Din (QN), Darbar Anayat shah (DA), Nathia Galli (NG), Kanhatti Garden (KG), Jaba (JB), Chok Azam (CA), Khanewal (KH)

Soil traits; Soil Ca^{2+}(OCa); Soil Mg^{2+} (OMg); Soil K^+, (OK); Soil Na^+ (ONa); Electrical conductivity (OEC); Soil pH (OpH); Soil organic matter (OOM); Soil saturation percentage (OSP)

Morphological traits; Shoot length (MSL); Root length (MRL); Shoot fresh weight (MSF); Root fresh weight (MRF); Shoot dry weight (MSD); Root dry weight (MRD)

Physiological traits: Proline (Pro); Glycine betaine (GB); Total soluble sugars (TSS); Shoot Na^+ (Na); Root Na^+ (RNa); Shoot Ca^{2+} (SCa); Root Ca^{2+} (RCa); Shoot K^+ (SK); Root K^+ (RK)

Physiological parameters: The maximum proline content (99.87 µmole g^{-1} fw) was noted in highly saline LS, while the minimum was in non-saline CA (13.25 µmole g^{-1} fw). The maximum glycine betaine content (119.25 µmole g^{-1} dw), total soluble sugars (59.42 µmole g^{-1} fw), and shoot Na^+ (58.75 mg g^{-1} dw) was observed in highly saline DF. The minimum concentration of glycine betaine (20.51 µmole g^{-1} dw), total soluble sugars (21.67 µmole g^{-1} fw) and shoot Na^+ (19.72 mg g^{-1} dw) was recorded in non-saline JB.

The maximum root Na^+ (84.74 mg g^{-1} dw) was noted in highly saline LD and the minimum (20.21 mg g^{-1} dw) was in non-saline KH. The maximum shoot calcium (30.71 mg g^{-1} dw) was recorded in highly saline DF and the minimum (11.25 mg g^{-1} dw) in non-saline JB. Root Ca^{2+} was the maximum (19.99 mg g^{-1} dw) in highly saline LS and the minimum (9.84 mg g^{-1} dw) in was recorded non-saline CA. The maximum shoot K^+ (30.15 mg g^{-1} dw) and root K^+ (32.42 mg g^{-1} dw) was noted in low saline KG. The minimum shoot K^+ (12.22 mg g^{-1} dw) was observed in highly saline LS, while root K^+ (9.31 mg g^{-1} dw) was the minimum in non-saline CA (Table 1).

Anatomical traits

Root anatomical parameters: The maximum root radius (1199.7 µm) was observed in low saline NG and the minimum (614.5 µm) was noted in highly saline DF. The maximum epidermis thickness (70.9 µm) was recorded in non-saline KH and the minimum (42.5 µm) was in low saline DA and KG and non-saline CA.

Cortical cell area was the maximum (5153.6 μm^2) in non-saline KH and the minimum (2050.9 μm^2) was in highly saline LD. The maximum endodermis thickness (75.6 µm) was observed in highly saline LS and LD, while the minimum (42.5 µm) was noted in low saline KG. The maximum endodermis cell area (1051.8 μm^2) was noted in low saline QN, and the minimum (420.7 μm^2) was in low saline KG.

Table 2. Root, Stem, leaf and leaf sheath characteristics of the collection sites of *Cenchrus ciliaris* L.

	High saline			Low saline				Non-saline		
	LS	**LD**	**DF**	**QN**	**DA**	**NG**	**KG**	**JB**	**CA**	**KH**
	Root anatomical traits									
RR (µm)	779.4g	651.8h	614.5i	803.3f	888.2e	1199.7a	1190.3b	769.9d	916.3d	939.9c
RET (µm)	66.1b	61.4c	47.2e	56.7d	42.5f	61.4c	42.5f	61.4c	42.5f	70.9a
RCC (µm^2)	3050.1g	2050.9j	3470.8e	3891.5d	2787.1h	3207.8f	4154.4c	4785.5b	2629.4i	5153.6a
RNT (µm)	75.6a	75.6a	56.7c	61.4b	56.7c	47.2d	42.5e	61.4b	56.7c	47.2d
RNC (µm^2)	841.4e	736.2f	946.6c	1051.8a	683.6g	999.2b	420.7j	473.3i	894.0d	578.5h
RMx (µm^2)	8098.5df	15197.9a	10359.8d	13988.3b	5889.8h	5679.5i	5942.4g	12726.2c	8519.2e	8939.9e
RPt (µm^2)	2629.4g	3681.1d	4838.1b	4312.2c	3102.7f	2208.7i	3365.6e	3891.5d	2471.6h	8519.2a
RPh (µm^2)	1788.1e	3260.4c	2471.6d	3891.5b	2313.9d	3155.3c	2366.4d	5101.0a	1367.3f	2313.9d
RAe (µm^2)	18616.3d	16985.8e	8887.3i	9150.2h	9413.2g	51535.9a	39651.1b	11569.3f	6731.3j	30395.7c
	Stem anatomical traits									
SET (µm)	56.7d	75.6a	66.1b	61.4c	66.1b	61.4c	61.4c	66.1b	42.5e	56.7d
SCC (µm^2)	5258.8c	3733.7g	4259.6e	3681.1h	6836.4a	2629.4j	3838.9f	4785.5d	6205.3b	3102.7i
SMx (µm^2)	3523.4d	5363.9a	3050.1f	2156.1h	4995.8b	3365.6e	2419.3g	3838.9c	1998.3i	3365.6e
SPh (µm^2)	3786.3g	4890.6d	3891.5f	4680.3e	5469.1c	3681.1h	5732.1a	5048.4b	2839.7j	3102.7i
SVN	37.6c	24.0g	19.0i	22.0h	37.0c	25.0f	30.0d	27.0e	45.0a	43b
SVA (µm^2)	32867.2e	58582.6a	31237.0f	19457.4h	19247.1i	44489.1b	38178.6c	35075.9d	28923.2g	31184.4f
SSc (µm)	56.7e	75.6c	56.7e	70.9c	56.7e	70.6d	70.9d	99.2a	47.2f	85.0b
SR (µm)	2333.3d	2338.1d	1218.6f	1119.4g	2541.2b	2475.3c	1648.4e	2602.6a	2489.2c	2352.2d
	Leaf anatomical traits									
LMd (µm)	382.6f	524.3b	496.2c	637.7a	458.2d	382.6f	396.8e	335.4h	382.6f	349.5g
LLm (µm)	259.8e	382.6a	307.3d	311.7c	340.1b	307.4d	259.8e	212.6g	382.6a	226.7f
LET (µm)	66.1b	66.1b	61.4c	75.6a	61.4c	61.4c	56.7d	47.2e	56.7d	42.5f
LCC (µm^2)	4259.6d	6783.8a	2313.9i	2366.4i	4732.9c	5469.1b	2682.2g	3260.4f	3512.5e	2524.2h
LMx (µm^2)	4207.3b	3050.1e	3102.7d	2787.1f	4207.4b	4312.2a	4207.3b	3838.9c	2313.9g	1262.1h
LPh (µm^2)	1998.3j	4207.2d	3050.1g	2629.4i	3418.2f	4101.8e	4995.8c	5048.4b	2944.9h	5784.6a
LBF (µm^2)	2313.9j	9097.7b	9676.2a	2471.7i	6100.2c	5942.4d	5784.7e	2576.8h	4838.1f	3891.5g
LSD	16.5f	16.3f	48.3a	12.6g	28.4d	36.1b	36.7b	32.2c	20.5e	36.3b
LSA (µm^2)	3770.9c	4363.0b	3178.9g	4877.6a	3288.2f	3461.2d	3361.0e	1862.7j	2126.8i	2705.2h
	Leaf sheath traits									
HET (µm)	56.7d	70.9a	42.5e	61.4c	56.7d	56.7d	66.1b	42.5e	70.9a	56.7d
HEC (µm^2)	2997.5d	2419.3f	3470.8b	5574.3a	3418.2c	2261.3g	2944.9d	2313.9f	2524.2e	2156.1h
HCC (µm^2)	6310.5f	22507.5a	5363.9g	16249.6b	10359.8c	16512.5b	7520.2e	4785.5h	3260.4i	9518.4d
HVA (µm^2)	7993.3g	20088.5e	31973.2c	23769.6d	20298.8e	15776.3f	38073.4b	5258.8h	25242.1d	48380.6a
HMx (µm^2)	2103.5h	3576.0b	3576.0b	2524.2f	2524.2f	4943.2a	2313.9g	2892.3d	2682.0e	3050.1c
HPh (µm^2)	3365.6d	5153.6b	4838.1c	3155.3e	2629.4h	6205.3a	5153.6b	3155.3e	3050.1f	2944.9g
HT (µm)	198.4f	935.2a	632.9d	812.4c	552.6e	878.5b	699.1d	595.1e	566.8e	623.5d

Highly saline LD showed the maximum (15197.9 µm^2) root metaxylem area, while the minimum (5679.5 µm^2) was noted in low saline NG. Non-saline KH showed the maximum (8519.2 µm^2) pith cell area and the minimum (2208.7 µm^2) was observed in low saline NG. The maximum phloem area (5101.0 µm^2) was observed in non-saline JB and the minimum (1367.3 µm^2) was in non-saline CA. The maximum root aerenchyma area (51535.9 µm^2) was observed in low saline NG and the minimum (6731.3 µm^2) was observed in non-saline CA (Table 2, Fig. 2).

Stem anatomical parameters: The maximum epidermis thickness (75.6 µm) was noted in highly saline LD and the minimum (42.5 µm) was in non-saline CA. The maximum cortical cell area (6836.4 µm^2) was observed in low saline DA and the minimum (2629.4 µm^2) was in low saline NG. Highly saline LD showed the maximum (5363.9 µm^2) metaxylem area, and the minimum (1998.3 µm^2) was noted in non-saline CA. The maximum phloem area (5732.1 µm^2) was observed in low saline KG, while the minimum (2839.7 µm^2) was recorded in non-saline CA. The maximum vascular bundle number (45.0) was observed in non-saline CA and the minimum (19.0) was in highly saline DF. Highly saline LD showed the maximum (58582.6 µm^2) vascular bundle area, while low saline DA showed the minimum (19247.1 µm^2) vascular bundle area. The maximum sclerenchyma thickness (99.2 µm) was noted in non-saline JB and the minimum (47.2 µm) in low saline CA. The maximum stem radius (2602.6 µm) was observed in non-saline JB, while the minimum (1119.4 µm) was noted in low saline QN (Table 2, Fig. 3).

Table 3. Pearson's correlation coefficients among soil, morph-physiological and anatomical attributes of *Cenchrus ciliaris* populations.

Characteristics	MSL	MRL	MSF	MRF	MSD	MRD
Soil physicochemical traits						
Electrical conductivity	-0.609	-0.587	-0.709	-0.445	-0.727	-0.697
pH	-0.477	-0.534	-0.471	-0.577	-0.504	-0.329
Soil Potassium	0.060	0.033	0.010	0.298	-0.016	-0.117
Soil Sodium	-0.654	-0.636	-0.747	-0.505	-0.767	-0.701
Soil Calcium	-0.519	-0.628	-0.619	-0.377	-0.648	-0.706
Soil Magnesium	-0.561	0.061	-0.522	-0.256	-0.457	-0.134
Organic matter	-0.030	-0.127	-0.111	-0.125	-0.101	0.002
Saturation percentage	0.387	0.502	0.438	0.391	0.494	0.751
Physiology						
Proline	-0.312	-0.645	-0.406	-0.268	-0.444	-0.522
Glycine betaine	-0.085	-0.561	-0.182	-0.117	-0.224	-0.379
Total soluble sugars	-0.339	-0.628	-0.415	-0.320	-0.451	-0.470
Shoot Na^+	-0.467	-0.565	-0.561	-0.308	-0.588	-0.584
Root Na^+	-0.442	-0.620	-0.549	-0.325	-0.579	-0.630
Shoot Ca^{2+}	-0.588	-0.664	-0.636	-0.488	-0.670	-0.538
Root Ca^{2+}	-0.538	-0.810	-0.596	-0.556	-0.634	-0.600
Shoot K^+	0.827	0.250	0.826	0.529	0.799	0.481
Root K^+	0.515	-0.169	0.479	0.286	0.441	0.182
Root anatomical traits						
Root radius	0.906	0.513	0.898	0.593	0.895	0.503
Epidermis thickness	-0.312	-0.198	-0.367	-0.172	-0.349	0.096
Epidermis cell area	0.012	-0.025	0.079	-0.031	0.104	0.021
Cortical cell area	-0.078	-0.224	0.023	-0.228	0.047	0.608
Endodermis thickness	-0.787	-0.369	-0.868	-0.425	-0.861	-0.722
Endodermis cell area	0.024	-0.164	-0.045	0.041	-0.086	-0.487
Metaxylem area	-0.752	-0.528	-0.745	-0.687	-0.735	-0.344
Pith cell area	-0.273	-0.282	-0.189	-0.393	-0.200	0.338
Phloem area	-0.212	-0.158	-0.189	-0.077	-0.144	0.363
Aerenchyma area	0.701	0.178	0.647	0.418	0.642	0.512
Stem anatomical traits						
Epidermis thickness	-0.316	-0.454	-0.360	-0.130	-0.356	0.162
Cortical cell area	-0.179	0.369	-0.156	0.170	-0.142	-0.318
Metaxylem area	-0.277	0.044	-0.363	0.195	-0.347	0.118
Phloem area	-0.078	-0.227	-0.066	-0.042	-0.056	0.146
Vascular bundle number	0.147	0.578	0.164	0.214	0.169	-0.017
Vascular bundle area	0.194	0.139	0.120	0.201	0.132	0.291
Sclerenchyma thickness	-0.144	-0.063	-0.104	-0.119	-0.056	0.593
Stem radius	0.188	0.768	0.127	0.578	0.175	0.277
Leaf anatomical traits						
Midrib thickness	-0.345	-0.629	-0.367	-0.435	-0.418	-0.491
Lamina thickness	0.063	0.124	-0.016	0.097	-0.052	-0.501
Epidermis thickness	-0.178	-0.478	-0.265	-0.198	-0.312	-0.695
Cortical cell area	0.069	0.242	-0.086	0.370	-0.080	-0.130
Metaxylem area	0.252	0.078	0.189	0.427	0.209	0.050
Phloem area	0.261	0.233	0.315	0.116	0.346	0.800
Bulliform cell area	0.069	-0.160	0.032	0.022	0.004	-0.004
Adaxial stomatal density	0.380	0.097	0.453	0.280	0.463	0.691
Adaxial stomatal area	-0.207	-0.661	-0.298	-0.331	-0.354	-0.491
Leaf sheath anatomical traits						
Epidermis thickness	0.186	0.122	0.120	-0.089	0.085	-0.419
Epidermis cell area	-0.252	-0.547	-0.221	-0.369	-0.264	-0.417
Cortical cell area	0.005	-0.253	-0.109	-0.009	-0.138	-0.069
Vascular bundle area	0.203	-0.156	0.280	-0.241	0.235	0.232
Metaxylem area	0.429	0.184	0.356	0.448	0.358	0.406
Phloem area	0.412	-0.161	0.335	0.155	0.322	0.144
Leaf sheath thickness	0.288	-0.069	0.260	0.051	0.245	0.282

Positively significant at p<0.05 | Positively significant at p<0.01
Negatively significant at p<0.05 | Negatively significant at p<0.01

Root anatomical traits: Root radius (RR); Epidermis thickness (RET); Cortical cell area (RCC); Endodermis thickness (RNT); Endodermis cell area (RNC); Metaxylem area (RMx); Pith cell area (RPt); Phloem area (RPh); Aerenchyma area (RAe)

Stem anatomical traits: Epidermis thickness (SET); Cortical cell area (SCC); Metaxylem area (SMx); Phloem area (SPh); Vascular bundle number (SVN); Vascular bundle area (SVA); Sclerenchyma thickness (SSc); Stem radius (SR)

Leaf anatomical traits: Midrib thickness (LMd); Lamina thickness (LLm); Epidermis thickness (LET); Cortical cell area (LCC); Metaxylem area (LMx); Phloem area (LPh); Bulliform area (LBF); Adaxial stomatal density (LSD); Adaxial stomatal area (LSA)

Leaf sheath anatomical traits: Epidermis thickness (HET); Epidermis cell area (HEC); Cortical cell area (HCC); Vascular bundle area (HVA); Metaxylem area (HMx); Phloem area (HPh); Leaf sheath thickness (HT)

Leaf anatomical parameters: The maximum midrib thickness (637.7 µm) was observed in low saline QN and the minimum (335.4 µm) was in non-saline JB. The maximum lamina thickness (382.6 µm) was observed in highly saline LD and non-saline CA, whereas the minimum (212.6 µm) was in non-saline JB. Low saline QN showed the maximum (75.6 µm) epidermis thickness, while non-saline KH showed the minimum (42.5 µm) epidermis thickness. The maximum parenchymatous cell area (6783.8 μm^2) was observed in highly saline LD and the minimum was in DF (2313.9 μm^2). Low saline NG showed the maximum metaxylem area (4312.2 μm^2) and the minimum (1262.1 μm^2) was recorded in non-saline KH. The maximum phloem area (5784.6 μm^2) was noted in non-saline KH and the minimum (1998.3 μm^2) was in highly saline LS. The maximum bulliform cell area (9676.2 μm^2) was observed in highly saline DF and the minim00um (2313.9 μm^2) was noted in highly saline population LS. Adaxial stomatal density was the maximum (48.3) in highly saline population DF, while the minimum in QN (12.6). Low saline QN showed the maximum adaxial stomatal area (4877.6 μm^2) and the minimum (1862.7 μm^2) was noted in non-saline JB (Table 2, Figs. 4 & 6).

Leaf sheath anatomical parameters: The maximum epidermis thickness (70.9 µm) was observed in highly saline LD, while the minimum was in DF (42.5 µm) and JB (42.5 µm). Low saline QN showed the maximum epidermis cell area (5574.3 μm^2), while the minimum (2156.1 μm^2) was recorded in non-saline KH. The maximum parenchyma cell area (22507.5 μm^2) was observed in highly saline LD and the minimum (3260.4 μm^2) was in non-saline CA. Non-saline KH showed the maximum vascular bundle area (48380.6 μm^2) and the minimum (5258.8 μm^2) was noted in non-saline JB. The maximum metaxylem area (4943.2 μm^2) was observed in low saline NG and the minimum (2103.5 μm^2) was in highly saline LS. Phloem area was the maximum (6205.3 μm^2) in low saline NG and the minimum (2629.4 μm^2) was noted in low saline DF. Highly saline LD showed the maximum leaf sheath thickness (935.2 µm) and the minimum (198.4 µm) was observed in highly saline LS (Table 2, Fig. 5).

Pearson's correlation coefficient: The correlation coefficient was calculated between morphology, soil and anatomical parameters at 0.05 and 0.01 levels of significance. Soil electrical conductivity showed negative correlation ($p<0.05$) with shoot fresh and dry weights and root dry weight. Soil Na^+ showed negative correlation ($p<0.05$) with shoot and root length, shoot fresh weight and root dry weight. Soil Ca^{2+} showed negative correlation ($p<0.05$) with root dry weight. Root dry weight showed positive correlation ($p<0.05$) with saturation percentage of soil (Table 3).

Proline showed negative correlation ($p<0.05$) with root length. Shoot K^+ showed positive correlation ($p<0.01$) with shoot length, shoot fresh weight and shoot dry weight. Shoot Ca^{2+} showed negative correlation ($p<0.05$) with root length, shoot fresh weight and shoot dry weight. Root Ca^{2+} showed negative correlation ($p<0.05$) with shoot dry weight and negative correlation ($p<0.01$) with root length.

Cenchrus ciliaris showed positive correlation ($p<0.05$) of shoot length, shoot fresh weight and shoot dry weight with root aerenchyma area. Root radius showed positive correlation ($p<0.01$) with shoot length, shoot fresh weight and shoot dry weight. Root endodermis thickness showed negative correlation ($p<0.01$) with shoot length, shoot fresh weight and shoot dry weight. Root metaxylem area showed negative correlation ($p<0.05$) with shoot length, root fresh weight and shoot dry weight.

Stem radius showed positive correlation ($p<0.01$) with root length. Leaf epidermis thickness showed negative correlation ($p<0.05$) with root dry weight. Leaf phloem area showed positive correlation ($p<0.01$) with root dry weight. Adaxial stomatal density positively correlated ($p<0.05$) with root dry weight, while adaxial stomatal area showed negative correlation ($p<0.05$) with root length. Root aand shoot Ca^{2+} showed negative correlation with root length, shoot fresh weight and shoot dry weight. Shoot K^+ positively correlated with shoot length, shoot fresh weight and shoot dry weight.

Multivariate analysis: Principal component analysis (PCA) biplot revealed a significant relationship among morphological and physiological traits with soil physicochemical characteristics. The first and second PCAs explained 55.2% and 20.1% variability among soil, morphological and physiological attributes. Soil OEc and ionic content (OCa and ONa) were strongly associated with shoot and root ionic content (RNa, RCa, SNa and SCa). Organic osmolytes like TSS, Prl and GB content did not show any association with soil or morphological parameters (Fig. 7a). The first and second PCAs explained 33.9% and 18.7% variability among soil and root anatomical traits. Soil OEC, OpH and ionic content (ONa and OCa) of DF and LS sites was strongly associated with RNT (Fig. 7b).

Principal component analysis showed 30.5% and 25.2% variations among soil and stem anatomical traits. Soil saturation percentage of JB site strongly affected the stem radius (Fig. 7c). The first and second PCAs showed 31.8% and 18.4% variability among soil and leaf anatomical traits. Soil (OSP) saturation percentage of KG site strongly associated with LSD, LPH and HVA. Soil organic matter of NG site showed strong association with Hph, LBF, LT, LCC and HMx. Soil K^+ (Ok) of site DA strongly associated with HEC (Fig. 7d).

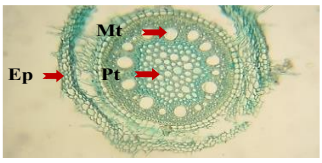

LS-Thin epidermis **(Ep)**; broad metaxylem vessels **(Mt)**; large pith parenchyma cells **(Pt)**

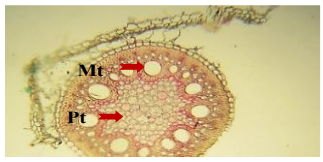

LD-Single-layered epidermis; large pith parenchyma cells **(Pt);** sclerified vascular region with broad metaxylem vessels **(Mt)**

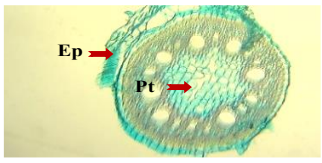

DF-Disintegrated epidermis **(Ep)**; broad metaxylem vessels; prominent pith cells **(Pt)**

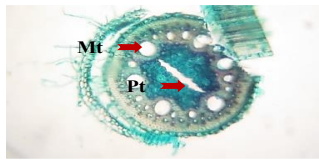

QN-Thick epidermis with small epidermal cells; prominent and large metaxylem vessels **(Mt)**; small pith cells **(Pt)** that disintegrated in the center

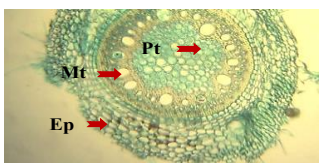

DA-Thin epidermis **(Ep)** multilayered; large cortical parenchymatous cells; thick endodermis; large metaxylem vessels **(Mt)**; large pith region **(Pt)**

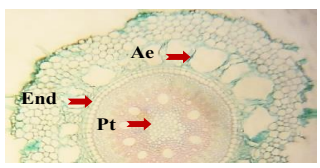

NG-Thick epidermis; large aerenchymatous cell in cortical region **(Ae)**; large metaxylem; reduced pith **(Pt)** ; prominent layer of endodermis **(End)**

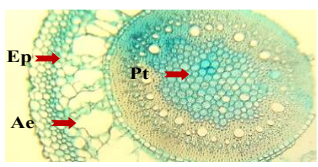

KG-Thick epidermis **(Ep)**; prominent small metaxylem; large aerenchymatous cell visible **(Ae)**; large pith parenchymatous cells **(Pt)**

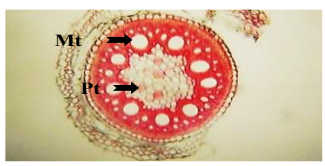

JB-Thick epidermis with small cells arrangement; large metaxylem vessels **(Mt)**; visible pith parenchymatous cells **(Pt)**; prominent endodermis; development of sclerenchyma tissue in vascular region

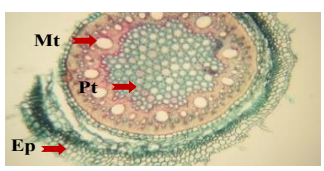

CA-Thick epidermis with small cells **(Ep)**; large metaxylem vessels **(Mt)**; prominent endodermis; large and prominent pith parenchymatous cells **(Pt)**

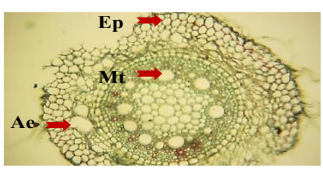

KH-Thick epidermis **(Ep)**; large aerenchymatous cells **(Ae)**; large pith parenchymatous cells; metaxylem vessels broad **(Mt)**; compactly arranged endodermis cells

Fig. 2. Root transverse sections of *Cenchrus ciliaris* L. collected from various saline habitats.
Highly saline: LS-Lal Suhanra LD-Ladamsar DF-Derawar Fort, Low saline: QN-Qila Nawab Din DA-Darbar Anayat Shah, NG-Nathia Galli, KG-Kanhatti Garden, Non saline: JB-Jaba, CA-Chok Azam, KH-Khanewal

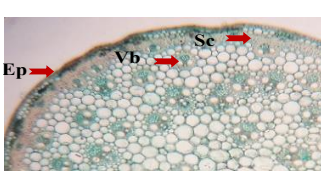

LS-Lignified epidermis **(Ep)**; prominent sclerenchyma **(Sc)**; small vascular bundles **(Vb)** arranged near the stem periphery, larger deeply inserted

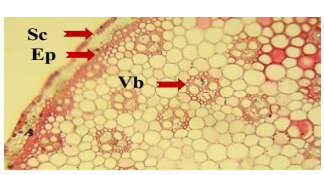

LD-Lignified epidermis of small cells **(Ep)**; sclerenchyma deposition **(Sc)**; large vascular bundles **(Vb)** with large metaxylem vessels

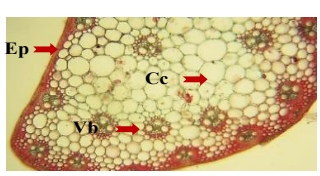

DF-Lignified thick epidermis **(Ep)**; prominent vascular bundle **(Vb)**; large cortical cells **(Cc)**; prominent metaxylem

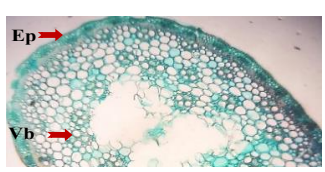

QN-Thick lignified epidermis **(Ep)** of small cells; scattered vascular bundles **(Vb)**

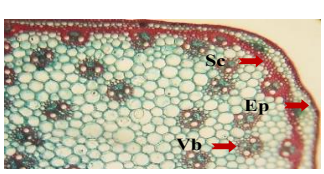

DA-Epidermis lignified **(Ep)**; sclerenchymatous deposition **(Sc)** inside distinctive hypodermis; scattered vascular bundles **(Vb)**

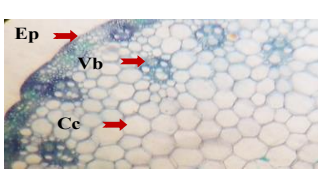

NG-Thick-layered epidermis **(Ep)**; scattered vascular bundles **(Vb)**; prominent metaxylem vessel; large cortical cells **(Cc)**

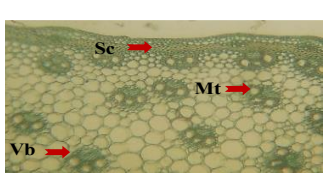

KG-Small epidermal cells; compact sclerenchymatous cells layer **(Sc)**; large metaxylem vessel **(Mt)** and vascular bundles **(Vb)**

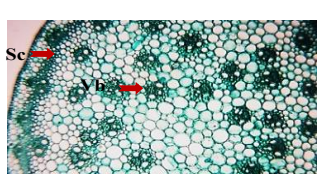

JB-Lignified epidermis; scleren-chymatous deposition **(Sc)**; small metaxylem; prominent vascular bundles **(Vb)**

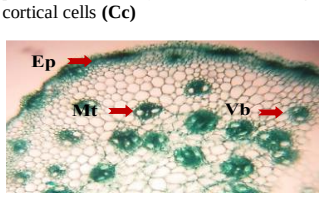

CA-Thick lignified epidermis **(Ep)**; scattered vascular bundles **(Vb)**; narrow metaxylem **(Mt)**; sclerfication in outer cortex

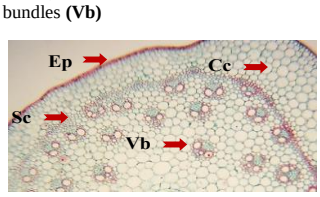

KH-Lignified epidermis **(Ep)**; large metaxylem vessel; prominent vascular bundles **(Vb)**; sclerenchyma deposition outside the vascular bundle **(Sc)**; large cortical cells **(Cc)**

Fig. 3. Stem transverse sections of *Cenchrus ciliaris* L. collected from various saline habitats.
Highly saline: LS-Lal Suhanra LD-Ladamsar DF-Derawar Fort, Low saline: QN-Qila Nawab Din DA-Darbar Anayat Shah, NG-Nathia Galli, KG-Kanhatti Garden, Non saline: JB-Jaba, CA-Chok Azam, KH-Khanewal

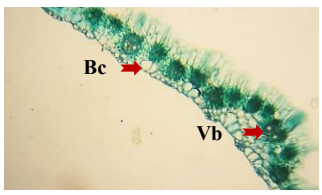

LS-Vascular bundle small **(Vb)**; prominent bulliform cell **(Bc)**; midrib thickness; reduced lamina thickness

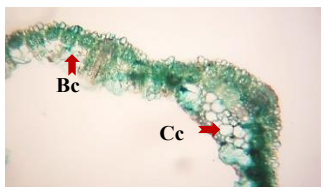

LD-Cortical cells prominent **(Cc)**; distinct bulliform cells **(Bc)**; vascular bundle at adaxial epidermis; thick epidermis

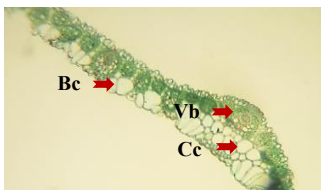

DF-Large adaxial epidermal cells; large vascular bundle **(Vb)**; large cortical cells **(Cc)** and bulliform cells **(Bc)**

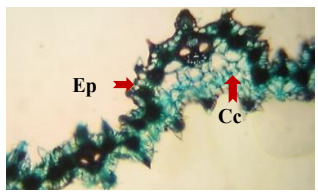

QN-Distinct metaxylem; thick adaxial epidermis **(Ep)**; large cortical cells **(Cc)**; thick midrib

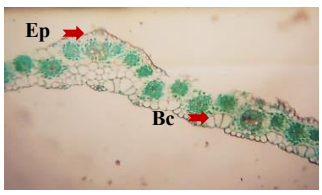

DA-Prominent adaxial epidermis **(Ep)**; small metaxylem; vascular bundle ring; distinct abaxial epidermis; distinct fan-shaped bulliform cells **(Bc)**

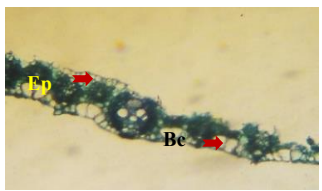

NG-Thick adaxial epidermis **(Ep)**; large metaxylem vessel; fan-shaped bulliform cells **(Bc)**

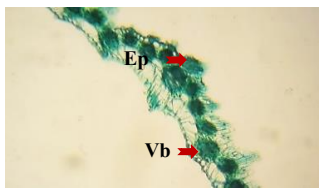

KG-Single layered epidermis **(Ep)**; small vascular bundles **(Vb)**

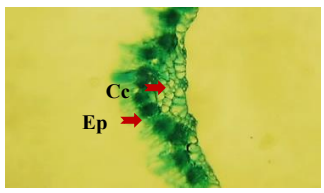

JB-Thick-layered epidermis **(Ep)**; large cortical cells **(Cc)** and bulliform cells

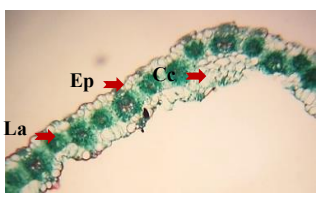

CA- Thick adaxial epidermis **(Ep)**; small metaxylem; large cells of abaxial epidermis; cortical cells large **(Cc)**; maximum lamina thickness **(La)**

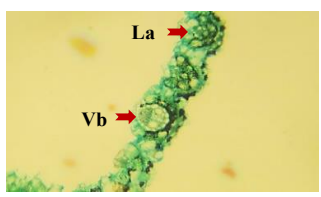

KH-Vascular bundles prominent **(Vb)**; large metaxylem vessels; reduced lamina thickness **(La)**

Fig. 4. Leaf transverse sections of *Cenchrus ciliaris* L. collected from various saline habitats.
Highly saline: LS-Lal Suhanra LD-Ladamsar DF-Derawar Fort, Low saline: QN-Qila Nawab Din DA-Darbar Anayat Shah, NG-Nathia Galli, KG-Kanhatti Garden, Non saline: JB-Jaba, CA-Chok Azam, KH-Khanewal

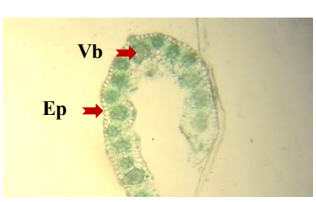

LS -Single layer epidermis **(Ep)**; small vascular bundles **(Vb)**

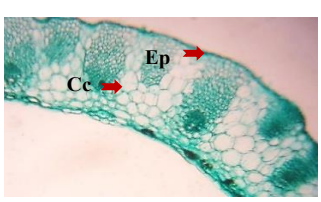

LD-Thin epidermis **(Ep)**; small vascular bundles; large cortical cell **(Cc)**

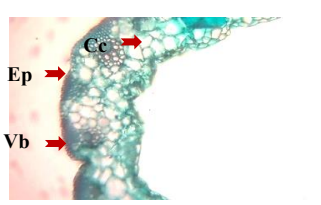

DF-Large cortical cells **(Cc)**; thick epidermis **(Ep)**; smaller vascular bundles **(Vb)**

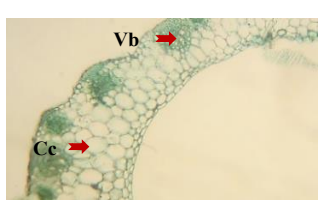

QN-Prominent vascular bundle **(Vb)**; large cortical cells **(Cc)**

DA-Prominent vascular bundles; large cortical cells **(Cc)**; sclerification outside vascular bundles **(Sc)**

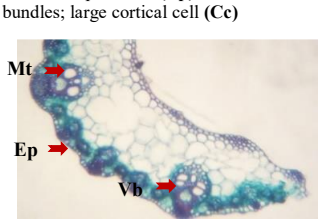

NG-Prominent metaxylem **(Mt)**; large vascular bundle **(Vb)**; thick adaxial epidermis **(Ep)**; large cortical cells **(Cc)**

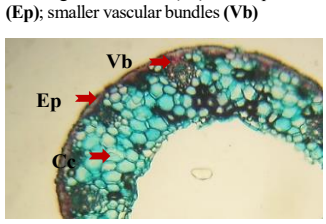

KG-Large cortical cells **(Cc)**; sclerified adaxial epidermis **(Ep)**; small metaxylem vessels and vascular bundle **(Vb)**

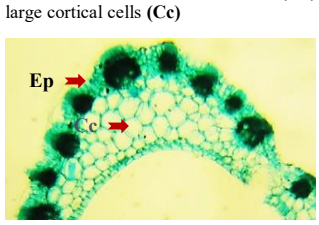

JB-Thick epidermis **(Ep)**; large cortex cells **(Cc)**

CA- Compact epidermis **(Ep)**; large vascular bundles **(Vb)**; large cortical cells **(Cc)**

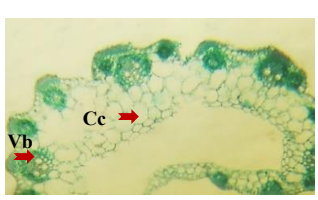

KH- Prominent vascular bundles **(Vb)**; cortical cells large **(Cc)**; small metaxylem vessels **(Mt)**

Fig. 5. Leaf sheath transverse sections of *Cenchrus ciliaris* L. collected from various saline habitats.
Highly saline: LS-Lal Suhanra LD-Ladamsar DF-Derawar Fort, Low saline: QN-Qila Nawab Din DA-Darbar Anayat Shah, NG-Nathia Galli, KG-Kanhatti Garden, Non saline: JB-Jaba, CA-Chok Azam, KH-Khanewal

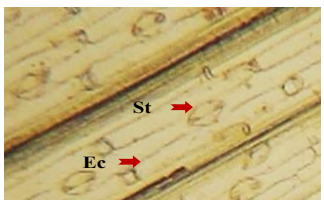

LS-Large elliptic stomata **(St)**; epidermal cell elongated **(Ec)**

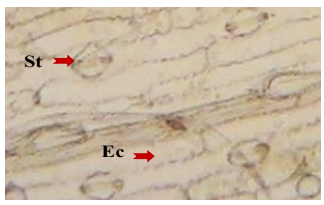

LD-Elongated epidermal cells **(Ec)**; stomata large, rhomboid **(St)**

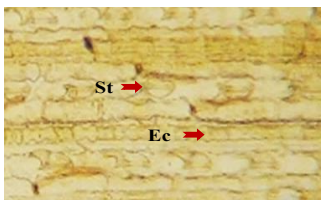

DF-Stomata numerous, circular **(St)**; epidermal cell with wavy cell walls **(Ec)**

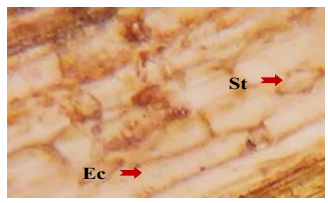

QN-Stomata narrowly elliptic **(St)**; epidermal cell broadly rectangular **(Ec)**

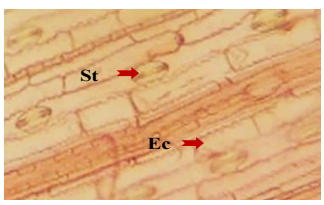

DA-Elongated epidermal cell **(Ec)**; Large elliptic stomata **(St)**

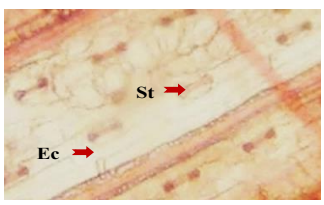

NG-Elongated epidermal cells **(Ec)**; narrowly elliptic stomata **(St)**

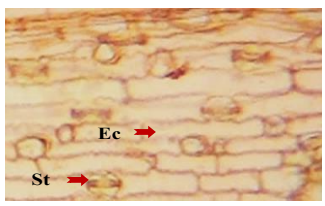

KG-Epidermal cells elongated **(Ec)**; with wavy margins, small circular stomata **(St)**

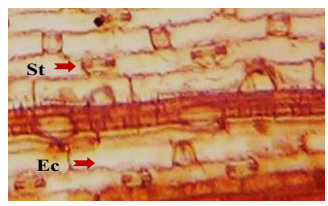

JB-Small circular stomata **(St)**; epidermal cell elongated **(Ec)** with wavy margins

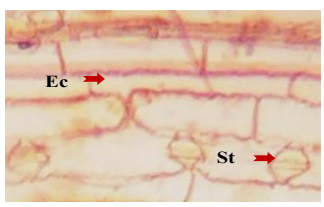

CA-Stomata **(St)** small, circular; elongated epidermal cells **(Ec)**

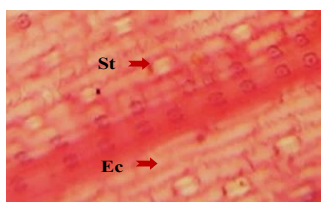

KH-Small, numerous stomata **(St)**, circular in shape; epidermal cell small **(Ec)**

Fig. 6. Epidermal surface view of *Cenchrus ciliaris* L. collected from various saline habitats.
Highly saline: LS-Lal Suhanra LD-Ladamsar DF-Derawar Fort, Low saline: QN-Qila Nawab Din DA-Darbar Anayat Shah, NG-Nathia Galli, KG-Kanhatti Garden, Non saline: JB-Jaba, CA-Chok Azam, KH-Khanewal

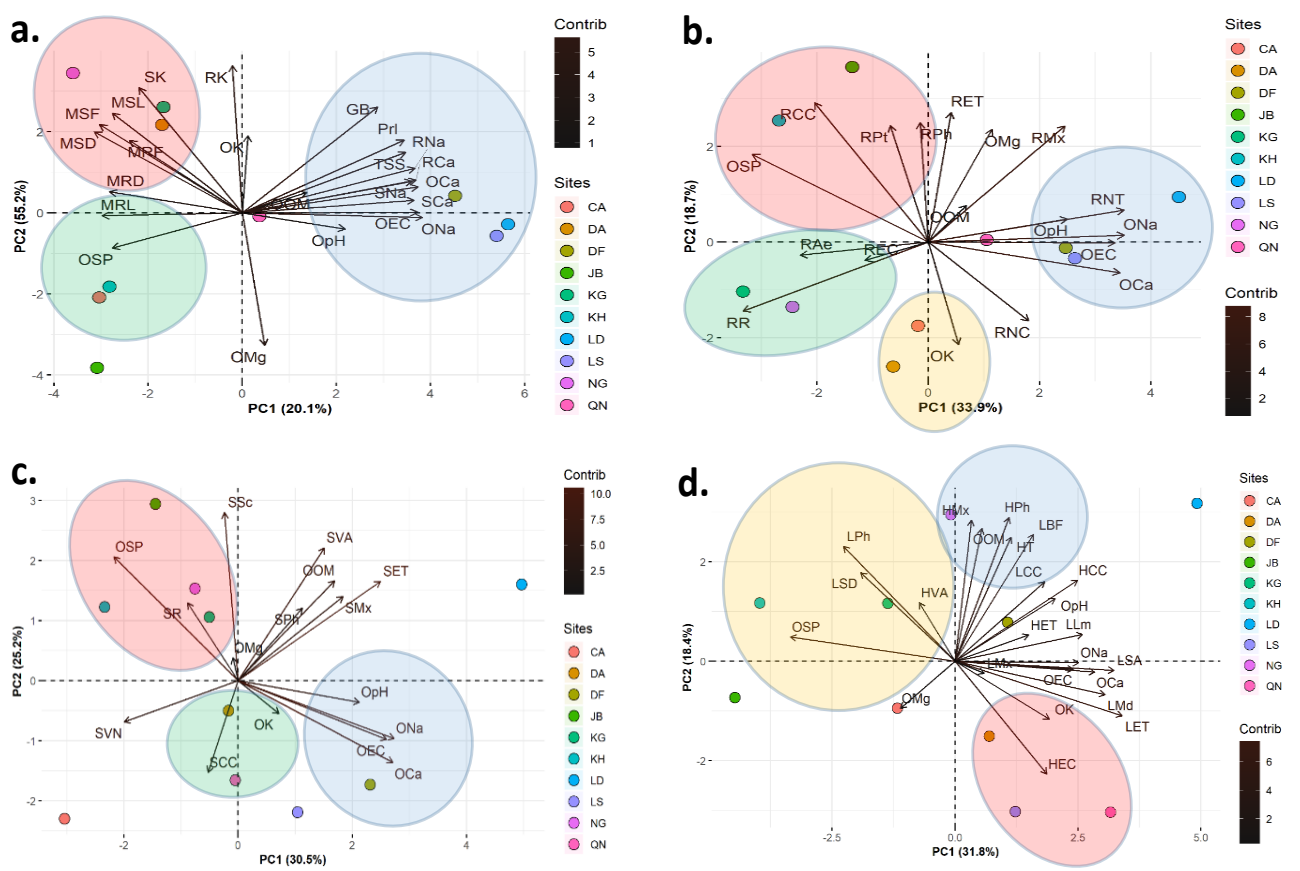

Fig. 7. Relationship between soil physicochemical characteristics with a) morphological and physiological attributes b) root anatomical traits c) Stem traits and d) leaf anatomical traits of *Cenchrus ciliaris* L.

Morphological traits; Shoot length MSL; Root length MRL; Shoot fresh weight MSF; Root fresh weight MRF; Shoot dry weight MSD; Root dry weight MRD; Physiological traits: Proline Pro; Glycine betaine GB; Total soluble sugars TSS; shoot Na^+ SNa; shoot Na^+ RNa; shoot Ca^{2+} SCa; root Ca^{2+} Ca RCa; shoot K^+ SK; root K^+ RK ; Root anatomical traits: Root radius RR; Epidermis thickness RET; Epidermis cell area REC; Cortical cell area RCC; Endodermis thickness RNT; Endodermis cell area RNC; Metaxylem area RMx; Pith cell area RPt; Phloem area RPh; Aerenchyma area Rae; Stem anatomical traits; Epidermis thickness SET; Cortical cell area SCC; Metaxylem area SMx; Phloem area SPh; Vascular bundle number SVN; Vascular bundle area SVA; Sclerenchyma thickness SSc; Stem radius SR; Leaf anatomical traits; Midrib thickness LMd; Lamina thickness LLm; Epidermis thickness LET; Cortical cell area LCC; Metaxylem area LMx; Phloem area LPh; Bulliform area LBF; Adaxial stomatal density LSD; Adaxial Stomatal Area LSA; Leaf sheath anatomical traits; Epidermis thickness HET; Epidermis cell area HEC; Cortical cell area HCC; Vascular bundle area HVA; Metaxylem area HMx; Phloem area HPh; Leaf sheath thickness HT; Soil traits; Soil Ca^{2+} OCa; Soil Mg^{2+} OMg; Soil K^+, OK; Soil Na^+ ONa; Electrical conductivity OEC; Soil pH OpH; Soil organic matter OOM; Soil saturation percentage OSP

Discussion

Populations of *Cenchrus ciliaris L.* collected from differently salt-affected soils in the Punjab region responded variably regarding morphological, physiological and anatomical attributes. This species is naturally adapted in saline and dryland areas all over Pakistan (Mansoor *et al.,* 2019).

Salt stress significantly affected shoot and root growth. In the present study, the highest shoot length and root length was observed in low saline populations. Alshammary *et al*., (2004) reported a reduction in shoot growth in Kentucky blue grass (*Poa pratensis* L.) and tall fescue (*Festuca arundinacea* Schreb.) under salt stress. In *C. ciliaris,* reduction in root length was recorded in high to moderately saline habitats. A considerable reduction in root length was noted by Ouji *et al*., 2015 in leguminous plants growing in saline conditions. Root length increased in some moderately saline habitats. Longer roots in plants can absorb more water and nutrients from deeper layers (Franco *et al*., 2011a).

In the current study, the maximum root fresh weight of *C. ciliaris* was observed from low to non-saline populations and the minimum shoot and root dry weights were observed from high saline populations. The reduction in vegetative growth is an important factor for the plants to survive under harsh environmental conditions as plants disburse their metabolic energy in survival rather than for normal vegetative growth (Mansoor *et al*., 2019).

In our investigation, the populations from high salinity accumulated higher concentration of proline, total soluble sugars and glycine betaine. Proline accumulation was first reported in ryegrass (*Lolium perenne* L.) in wilting condition (Kemble & Macpherson, 1954). It accumulates in cytoplasm, where it acts as an osmoprotectant to defend against osmotic stress (Meena *et al*., 2019). Glycine betaine and total soluble sugars are also accumulated in populations colonizing high salinities for osmoprotection (Kosar *et al*., 2018).

Root and shoot Na^+ and Ca^{2+} were significantly higher in the populations from highly saline habitats. Root and shoot Na^+ is generally proportional to salinity level of the habitats (Abbas *et al.,* 2018) as was the case with *C. ciliaris* in the present study. The increased Na^+ concentration was neutralized by increased uptake of Ca^{2+} (Chelli-Chaabouni *et al.,* 2010). In plants, calcium provides structural stability and act as a signaling molecule but higher concentration of toxic salts reduced the uptake of Ca^{2+} (Ali *et al*., 2021).

Populations collected from various habitats showed enormous variation in root anatomical parameters. Epidermis was more developed in the non-saline KH population (forest plantation) and LS population (saline desert). In salt affected soils, epidermis act as an obstacle, which restricts the influx of ions toxic for plants. It is a critical feature of plants to prevent the surface water loss in dry environment (Yuan *et al*., 2016). Earlier studies also reported thick epidermis in saline arid region plants (Liu *et al*., 2015) which plays a vital role in evapo-transpiration of water.

Cortical cell area was the maximum in KH (forest plantation) and JB population (mountain slopes along the road), that are relatively drier regions. Cortical parenchyma plays a vital role in storage of additional water for their survival in harsh environmental conditions (Grigore & Toma, 2007). Toxic salts and water are more efficiently stored in large sized cortical cells as compared to smaller ones (Chimungu *et al*., 2015).

Thick root endodermis was observed in LS (saline desert) and LD (Cholistan Desert) populations. Endodermal layer acts as protective covering and prevents uptake of toxic ions, limits loss of water from roots and helps to conserve water (Paez-Garcia *et al*., 2015). Under harsh environmental conditions, an increase in endodermal thickness ensures the survival of species and also checks water loss though root (Naz *et al*., 2018). Metaxylem area was more developed in LD population from Cholistan Desert. Under saline and arid conditions, larger metaxylem vessels help in the maximum translocation of water and nutrients are positively correlated with hydraulic conductivity (Smith *et al*., 2013).

The maximum phloem area was observed in non-saline JB population (mountain slopes along the road). Ahmad & Amanullah (2016) reported an increase in phloem area, which was positively correlated with translocation of photo-assimilates. It is critical for survival of plants under salt stress conditions (Lemoine *et al*., 2013).

Root aerenchyma area was maximum in low saline NG population (mountainous region). Root aerenchymatous area is a vital feature of marshy halophytes. In saline areas, it is an adaptive component in grasses (Grigore *et al*., 2014). It permits plants to survive in waterlogged and saline conditions which is an adaptive component in grasses (Lacramioara *et al*., 2015). In roots, aerenchyma tissues enable plants to maintain their oxygen requirement (Al-Hassan *et al*., 2015). Grasses of high altitude showed distinctly enlarged aerenchyma and more intense sclerification than that those of low altitude populations, specifically in the outer cortex and pith region (Ahmad *et al*., 2016).

The maximum stem epidermal thickness was noted in highly saline LD population (Cholistan Desert) and DA low saline population (scattered sand dunes in Thal Desert). It enables the plants to survive in harsh water deficit environments, to retain moisture in tissues (Bartoli *et al*., 2015). Epidermis acts as protective covering, which conserves water during stress conditions (Shimamura *et al*., 2010).

Large cortical cells were developed in DA population (scattered sand dunes) and CA population (Thal Desert). Cortical region plays a vital role in plant functioning. It acts as a storage house for nutrients and water. In stressful conditions such as water deficit and salinity, large cortical cell area increases the survival success of plants (Shafi *et al*., 2015).

Highly saline LD population (Cholistan Desert) and low saline DA population (scattered sand dunes) showed the maximum metaxylem area in stem. At high salinity, increase in vascular tissues mainly metaxylem area in *C. ciliaris* is involved to minimize resistant in conduction that may enhance transport of water and nutrients (Horie *et al*., 2012).

Vascular bundle number was more in CA (Thal Desert) and KH population (forest plantation). Vascular bundles are involved in water and minerals conduction and also provide mechanical strength (Notaguchi & Okamoto, 2015). Any decrease in vascular bundle size affects the conduction of water, solutes and photosynthates that ultimately results in decreased plant growth (Zhaosen *et al*., 2014). Highly saline LD population (Cholistan Desert) and NG population (cool mountainous region) showed maximum vascular bundle area while low saline QN (Cholistan Desert flats) and DA (scattered sand dunes) populations showed minimum vascular bundle area. Vascular bundles are the vital element of the internal anatomy of plants (Zhaosen *et al*., 2014). Under high salinity increased vascular bundle area was reported by Naz *et al*., (2013) in different populations of *Aeluropus lagopoides*.

Sclerenchyma thickness was the maximum in non-saline JB (mountain slopes along the road) and KH (forest plantation) and the minimum in LS and DF (high saline) and CA (non-saline) populations. This feature may prevent loss of water under salinity stress (Naz *et al*., 2018). Sclerification is a characteristic of grasses colonizing in arid/semi-arid and salt-affected areas (Fatima *et al*., 2018). These cells are mechanical tissues (Al-Maskri *et al*., 2014) and under osmotic stress conditions like salinity, they provide mechanical strength to the plants (Nawaz *et al*., 2013).

Leaves are more sensitive to environmental stresses than other organs of plants (Ali *et al*., 2009). At leaf level, the maximum midrib thickness was observed in QN (Cholistan Desert flats) and LD population (Cholistan Desert). The maximum lamina thickness was observed in highly saline as compared to non-saline populations. The more lamina thickness means the more layers of mesophyll cells to carry out Photosynthesis (Bano *et al*., 2019). Increase in lamina and midrib thickness is a stress response in plants under salinity (Naz *et al*., 2022). Increase in leaf blade thickness and bulliform cells under harsh environmental conditions is acute adaptation in grasses against oxidative as well as salt stresses (Ahmad *et al*., 2015).

Leaf epidermis thickness was the maximum in QN (Cholistan Desert flats), LS (saline desert) and LD population (Cholistan Desert). During limited moisture availability, thick epidermis is a valuable attribute to check water loss (Liu *et al*., 2015). Thick epidermis acts as a hurdle, which prevents loss of water and thus helps to conserve water (Ma *et al*., 2012).

Low saline NG (mountainous region), KG (gravel stones and scrub vegetation) and DA population (scattered sand dunes) showed broad metaxylem vessels. Under salt stress conditions increase in metaxylem area is an adaptive feature, which is reported by Correa *et al*., (2015) in cattail.

Bulliform cell area was the maximum in highly saline DF (muddy flats, heavily salt-affected) and LD population (Cholistan Desert). Bulliform cells are not only involved in leaf rolling during stress condition but also aid to conserve water loss through leaf surface (Mansoor *et al*., 2019). In *C. ciliaris,* this might be an important adaptation and defensive feature, when growing under salinity (Ahmad *et al*., 2015).

Adaxial stomatal density was the maximum in highly saline DF (muddy flats, heavily salt affected), NG (cool mountainous region) and KG (gravel stones and scrub vegetation) populations. Smaller and large numbers of stomata are easier to maintain turgor at lower water potential, which is again an adaptive feature of populations inhabiting saline areas (Fatima *et al.,* 2021). Adaxial stomatal area was the maximum in QN (Cholistan Desert flats) and LD population (Cholistan Desert). Modification in stomatal structures is a critical modification during saline conditions that lowers the transpiration rate (Camargo & Marenco, 2011). Stomatal density and size is also very important for controlling rate of transpiration when water is a vital commodity (Rahat, 2019). A decrease in adaxial stomatal density and size reduces water loss through transpiration (Naz *et al*., 2010).

One of the prominent anatomical attributes was increase in leaf sheath thickness at highly saline LD (Cholistan Desert) and low saline NG (mountainous) region. The increase in leaf sheath thickness was due to high proportion of storage parenchyma. Increased parenchyma area is linked to storage potential under salinity stress (Akcin *et al*., 2017). Plants growing in highly saline area LD (Cholistan Desert) and CA (Thal desert) had the maximum epidermis thickness (Table 2). Plants under hot hypersaline and arid climatic conditions tend to develop thick epidermis in order to protect internal tissues from external harsh environmental conditions (Fatima *et al*., 2021).

Conclusion

It is concluded that buffel grass (*Cenchrus ciliaris* L.) has the ability to survive and tolerate high and moderate salinity levels. It also develops crucial anatomical modifications such as formation of root and leaf sheath aerenchyma, sclerification in stem and more developed bulliform cells in leaf blade. At root level, in saline areas formation of root aerenchyma is an adaptive strategy which ensures maximum water translocation along with toxic ions. At leaf level, the formation of bulliform cells in leaf blade ensures the maximum water storage and also prevents from desiccation by rolling and unrolling of leaves. At stem level, high proportion of sclerenchyma prevents loss of water under salinity stress. In *C. ciliaris,* anatomical modifications are vital for water conservation. Great variation in structural and functional features in *C. ciliaris* could be a strong reason for their distribution in various environmental conditions. This grass species can be cultivated in barren and saline areas and can be used as forage grass because of its high nutritional value.

References

Abbas, T., M. Rizwan, S. Ali, M. Adrees, A. Mahmood, M. Zia-ur-Rehman and M.F. Qayyum. 2018. Biochar application increased the growth and yield and reduced cadmium in drought stressed wheat grown in an aged contaminated soil. *Ecotoxicol. Environ. Saf.,* 148: 825-833.

Ahmad, F., M. Hameed, K. S. Ahmad and M. Ashraf. 2015. Significance of anatomical markers in tribe Paniceae (Poaceae) from the Salt Range. Pakistan. *Int. J. Agric. Biol.,* 17: 271-279.

Ahmad, I. and S. Amanullah. 2016. Effectiveness of various salinity on leaf growth of Gazania. *Int. J. Agron.,* 9: 1-9.

Ahmad, K. S., M. Hameed, S. Fatima, M. Ashraf, F. Ahmad, M. Naseer and N. Akhtar. 2016. Morpho-anatomical and physiological adaptations to high altitude in some Aveneae grasses from Neelum Valley, Western Himalayan Kashmir. *Acta Physiol. Plant.,* 38: 1-14.

Akcin, T.A., A. Akcin and E. Yalcin. 2017. Anatomical changes induced by salinity stress in *Salicornia freitagii* (Amaranthaceae). *Rev. Bras. Bot.,* 40: 1013-1018.

Al-Dakheel, A. J., M. I. Hussain and A. Q. M. A. Rahman. 2015b. Impact of irrigation water salinity on agronomical and quality attributes of *Cenchrus ciliaris* L. accessions. *Agric. Water Manag*., 159: 148-154.

Ali, M., S. Afzal, A. Parveen, M. Kamran, M.R. Javed, G.H. Abbasi and S. Ali. 2021. Silicon mediated improvement in the growth and ion homeostasis by decreasing Na^+ uptake in maize (*Zea mays* L.) cultivars exposed to salinity stress. *Plant Physiol. Biochem.,* 158: 208-218.

Al-Maskri, A., M. Hameed, M. Ashraf, M. M. Khan, S. Fatima, T. Nawaz and R. Batool. 2014. Structural features of some wheat (*Triticum* spp.) landraces/cultivars under drought and salt stress. *Arid Land Res. Manag.,* 28: 355-370.

Alshammary, S. F., Y. L. Qian and S.J. Wallner. 2004. Growth response of four turfgrass species to salinity. *Agric. Water Manag.,* 66: 97-111.

Bano, C., N. Amist and N.B. Singh. 2019. Molecular Plant Abiotic Stress: Biology and Biotechnology, In: (Eds.): Roychoudhury, A. and D. Tripathi. Morphological and Anatomical Modifications of Plants for Environmental Stresses. Wiley Online Liberary, pp. 29-44.

Bartoli, G., L. M. Forino, M. Daurante and A. M. Tagliasacchi. 2015. A lysigenic programmed cell death-dependent process shapes schizogenously formed aerenchyma in the stems of the waterweed *Egeria densa*. *Ann. Bot.,* 116: 91-99.

Bates, L.S., R.P. Waldren and I.D. Teare. 1973. Rapid determination of free proline for water-stress studies. *Plant Soil,* 39: 205-207.

Camargo, M.A.B. and R.A. Marenco. 2011. Density, size and distribution of stomata in 35 rainforest tree species in Central Amazonia. *Acta Amazon.*, 41: 205-212.

Chelli-Chaabouni, A., A.B. Mosbah, M. Maalej, K. Gargouri, R. Gargouri-Bouzid and N. Drira. 2010. *In vitro* salinity tolerance of two pistachio rootstocks: *Pistacia vera* L. and *P. atlantica* Desf. *Environ. Exp. Bot.,* 69: 302-312.

Chimungu, J.G., K.W. Loades and J.P. Lynch. 2015. Root anatomical phenes predict root penetration ability and biomechanical properties in maize (*Zea mays*). *J. Exp. Bot.,* 66: 3151-3162.

Correa, F. F., R.H. Madail, S. Barbosa, M.P. Pereira, E.M. Castro, C.T.G. Soriano and F.J. Pereira. 2015. Anatomy and physiology of cattail as related to different population densities. *Planta Daninh.,* 33: 1-12.

Estefan, G., R. Sommer and J. Ryan. 2013. Methods of soil, plant and water analysis: A manual for the West Asia and North Africa region. The International Center for Agricultural Research in the Dry Areas, (3rd ed.,), pp.1-243.

Fatima, S., M. Hameed, F. Ahmad, M. Ashraf and R. Ahmad. 2018. Structural and functional modifications in a typical arid zone species *Aristida adscensionis* L. along altitudinal gradient. *Flora*, 249: 172-182.

Fatima, S., M. Hameed, N. Naz, S.M.R. Shah, M. Naseer, M.S.A. Ahmad and I. Ahmad 2021. Survival strategies in khavi grass [*Cymbopogon jwarancusa* (Jones) Schult.] colonizing hot hypersaline and arid environments. *Water Air Soil Pollut*., 232: 1-17.

Franco, J.A., V. Cros, M.J. Vicente and J.J. Martinez-Sanchez. 2011a. Effects of salinity on the germination, growth, and nitrate contents of purslane (*Portulaca oleracea*) cultivated under different climatic conditions. *J. Hort. Sci. Biotechnol.,* 86: 1-6.

Grieve, C.M. and S.R. Grattan. 1983. Rapid assay for determination of water soluble quaternary ammonium compounds. *Plant Soil,* 70: 303-307.

Grigore, M.N. and C. Toma. 2007. Histo-anatomical strategies of Chenopodiaceae halophytes: Adaptive, ecological and evolutionary implications. *WSEAS Trans. Biol*. *Biomed.,* 4: 204-218.

Grigore, M.N., L. Ivanescu and C. Toma. 2014. Halophytes: an integrative anatomical study. Springer.

Hameed, M., T. Nawaz, M. Ashraf, N. Naz, R. Batool, M. S. A. Ahmad and A. Riaz. 2013. Physio anatomical adaptations in response to salt stress in *Sporobolus arabicus* (Poaceae) from the Salt Range, Pakistan. *Turk. J. Bot.,* 37: 715-724.

Horie, T., I. Karahara and M. Katsuhara. 2012. Salinity tolerance mechanisms in glycophytes: An overview with the central focus on rice plants. *Rice,* 5: 1-18.

Hussain, S., M. Shaukat, M. Ashraf, C. Zhu, Q. Jin and J. Zhang. 2019. Salinity stress in arid and semi-arid climates: Effects and management in field crops. In: (Ed.): Hussain, S. Climate Change and Agriculture, *IntechOpen*, pp. 13.

Kemble, A.R. and H.T. Macpherson. 1954. Liberation of amino acids in perennial rye grass during wilting. *Biochem. J.,* 58: 46-49.

Khan, M.A., Z. Abideen, M.Y. Adnan, S. Gulzar, B. Gul, M. Rasheed and M. Qasim. 2017. Antioxidant properties, phenolic composition, bioactive compounds and nutritive value of medicinal halophytes commonly used as herbal teas. *S. Afr. J. Bot.,* 110: 240-250.

Kosar, F., N.A. Akram, M. Ashraf, M. Sadiq and F. Al-Qurainy. 2018. Trehalose-induced improvement in growth, photosynthetic characteristics and levels of some key osmoprotectants in sunflower (*Helianthus annuus* L.) under drought stress. *Pak. J. Bot.,* 50: 955-961.

Lacramioara, O., M.N. Grigore and G. Vochita. 2015. Impact of saline stress on growth and biochemical indices of *Calendula officinalis* seedlings. *Rom. Biotechnol. Lett.,* 20: 11007-11017.

Lemoine, R., S.L. Camera, R. Atanassova, F. Dédaldéchamp, T. Allario, N. Pourtau and M. Durand. 2013. Source-to-sink transport of sugar and regulation by environmental factors. *Front. Plant Sci.,* 4: 272.

Liu, Y., X. Li, G. Chen, M. Li, M. Liu and D. Liu. 2015. Epidermal micromorphology and mesophyll structure of *Populus euphratica* heteromorphic leaves at different development stages. *PLoS One,* 10: e0137701.

Ma, H., H. Yang, X. Lu, Y. Pan, H. Wu, Z. Liang and M.K. Ooi. 2015. Does high pH give a reliable assessment of the effect of alkaline soil on seed germination? A case study with *Leymus chinensis* (Poaceae). *Plant Soil,* 394: 35-43.

Ma, J., C. Ji, M. Han, T. Zhang, X. Yan, D. Hu and J. He. 2012. Comparative analyses of leaf anatomy of dicotyledonous species in Tibetan and Inner Mongolian grasslands. *Sci. China Life Sci.,* 55: 68-79.

Ma, X., J. Zheng, X. Zhang, Q. Hu and R. Qian. 2017. Salicylic acid alleviates the adverse effects of salt stress on *Dianthus superbus* (Caryophyllaceae) by activating photosynthesis, protecting morphological structure, and enhancing the antioxidant system. *Front. Plant Sci.,* 8: 600.

Mansoor, U., S. Fatima, M. Hameed, M. Naseer, M.S.A. Ahmad, M. Ashraf and M. Waseem 2019. Structural modifications for drought tolerance in stem and leaves of *Cenchrus ciliaris* L., populations from the Cholistan Desert. *Flora*, 261: 151485.

Meena, M., K. Divyanshu, S. Kumar, P. Swapnil, A. Zehra, V. Shukla and R.S. Upadhyay. 2019. Regulation of L-proline biosynthesis, signal transduction, transport, accumulation and its vital role in plants during variable environmental conditions. *Heliyon*, 5:1-20.

Mumtaz, S., M.H. Saleem, M. Hameed, F. Batool, A. Parveen, S. F. Amjad, A. Mahmood, M. Arfan, S. Ahmed, H. Yasmin, A.A. Alsahli and M.N. Alyemeni. 2021. Anatomical adaptations and ionic homeostasis in aquatic halophyte *Cyperus laevigatus* L. under high salinities. *Saudi J. Biol. Sci*., 28: 2655-2666.

Nawaz, T., M. Hameed, M. Ashraf, S. Batool and N. Naz. 2013. Modifications in root and stem anatomy for water conservation in some diverse blue panic (*Panicum antidotale* Retz.) Populations under drought stress. *Arid Land Res. Manag.,* 27: 286-297.

Naz, N., M. Hameed, T. Nawaz, R. Batool, M. Ashraf, F. Ahmad and T. Ruby. 2013. Structural adaptations in the desert halophyte *Aeluropus lagopoides* (Linn.) Trin. ex Thw. under high salinity. *J. Biol. Res.,* 19: 150-164.

Naz, N., M. Hameed., M. Ashraf, F. AL-Qurainy and M. Arshad. 2010. Relationships between gas-exchange characteristics and stomatal structural modifications in some desert grasses under high salinity. *Photosynthetica,* 48: 446-456.

Naz, N., S. Fatima, M. Hameed, F. Ahmad, M.S.A. Ahmad, M. Ashraf, H. Shahid, U. Iqbal, M. Kaleem, S.M.R. Shah and I. Ahmad. 2022. Modulation in plant micro-structures through soil physicochemical properties determines survival of *Salsola imbricata* Forssk. in hypersaline environments. *J. Soil Sci. Plant Nutr.,* 22: 861-881.

Naz, N., S. Fatima, M. Hameed, M. Ashraf, M. Naseer, F. Ahmad and A. Zahoor. 2018. Structural and functional aspects of salt tolerance in differently adapted Populations of *Aeluropus lagopoides* from saline desert habitats. *Int. J. Agric. Biol*., 20: 41-51.

Negrao, S., S.M. Schmockel and M. Tester. 2017. Evaluating physiological responses of plants to salinity stress. *Ann. Bot.,* 119: 1-11.

Notaguchi, M. and S. Okamoto. 2015. Dynamics of long-distance signaling via plant vascular tissues. *Front. Plant Sci.,* 6:1-10.

Ouji, A., S. El-Bok, M. Mouelhi, M. B. Younes and M. Kharrat. 2015. Effect of salinity stress on germination of five Tunisian lentil (*Lens culinaris* L.) genotypes. *Eur. Sci. J.,* 11: 63-75.

Paez-Garcia, A., C.M. Motes, W. Scheible, R. Chen, E.B. Blancaflor and M.J. Monteros. 2015. Root traits and phenotyping strategies for plant improvement. *Plants*, 4: 334-355.

Rahat, Q.U.A. 2019. Morpho-anatomical and physiological adaptations in *Leptochloa fusca* from different ecological zones (Doctoral dissertation, University of Agriculture, Faisalabad).

Robbins, N.E., P. Aggarwal, Y. Bao, C.J. Sturrock, M.C. Thompson, H.Q. Tan and J.R. Dinneny. 2014. Plant roots use a patterning mechanism to position lateral root branches toward available water. *Proc. Natl. Acad. Sci.,* 111: 9319-9324.

Safdar, H., A. Amin, Y. Shafiq, A. Ali, R. Yasin, A. Shoukat and M.I. Sarwar. 2019. A review: Impact of salinity on plant growth. *Nat. Sci.,* 17: 34-40.

Shafi, A., R. Chauhan, T. Gill, M.K. Swarnkar, Y. Sreenivasulu, S. Kumar, N. Kumar, R. Shankar, P.S. Ahuja and A.K. Singh. 2015. Expression of SOD and APX genes positively regulates secondary cell wall biosynthesis and promotes plant growth and yield in *Arabidopsis* under salt stress. *Plant Mol. Biol.,* 87: 615-631.

Shimamura, S.R., T. Yamamoto, S. Nakamura S. Shimada and S. Komatsu. 2010. Stem hypertrophic lenticels and secondary aerenchyma enable oxygen transport to roots of soybean in flooded soil. *Ann. Bot.,* 106: 277-284.

Shrivastava, P. and R. Kumar. 2015. Soil salinity: A serious environmental issue and plant growth promoting bacteria as one of the tools for its alleviation. *Saudi J. Biol. Sci.,* 22: 123-131.

Sims, J.R. and V. A. Haby. 1971. Simplified colorimetric determination of soil organic matter. *Soil Sci.,* 112: 137-141.

Smith, M.S., J.D. Fridley, J. Yin and T.L. Bauerle. 2013. Contrasting xylem vessel constraints on hydraulic conductivity between native and non-native woody understory species. *Front. Plant Sci.,* 4: 486.

Wolf, B. 1982. A comprehensive system of leaf analyses and its use for diagnosing crop nutrient status. *Comm. Soil Sci. Plant Anal.,* 13: 1035-1059.

Xu, C. and B. Mou. 2015. Evaluation of lettuce genotypes for salinity tolerance. *Hort. Sci.,* 50: 1441-1446.

Yemm, E.W. and A. Willis. 1954. The estimation of carbohydrates in plant extracts by anthrone. *Biochem. J.,* 57: 508-514.

Yuan, F., B. Leng and B. Wang. 2016. Progress in studying salt secretion from the salt glands in recretohalophytes: how do plants secrete salt? *Front. Plant Sci.,* 7: 977.

Zhaosen, X., C.F. Forney, C. Hongmei and B. Li. 2014. Changes in water translocation in the vascular tissue of grape during fruit development. *Pak. J. Bot.,* 46: 483-488.

(Received for publication 24 March 2022)